Journal of Oceanology and Limnology
Vol. 36 No. 3, P. 612-619, 2018
https://doi.org/10.1007/s00343-018-7087-8

Effect of mesoscale wind stress-SST coupling on the Kuroshio extension jet*

WEI Yanzhou (魏艳州)[1,2], ZHANG Ronghua (张荣华)[1,2,3,**], WANG Hongna (王宏娜)[1,3], KANG Xianbiao (康贤彪)[4]

[1] *Key Laboratory of Ocean Circulation and Waves, Institute of Oceanology, Chinese Academy of Sciences, Qingdao 266071, China*

[2] *University of Chinese Academy of Sciences, Beijing 100049, China*

[3] *Qingdao National Laboratory for Marine Science and Technology, Qingdao 266000, China*

[4] *College of Air Traffic Management, Civil Aviation Flight University of China, Guanghan 618307, China*

Received Mar. 24, 2017; accepted in principle Apr. 6, 2017; accepted for publication Apr. 11, 2017

Abstract Effect of mesoscale wind stress-SST coupling on the Kuroshio extension jet is studied using the Regional Ocean Modeling System. The mesoscale wind stress perturbation (τ_{MS}) is diagnostically determined from modelled mesoscale SST perturbation (SST_{MS}) by using their empirical relationship derived from corresponding observation. From comparing two experiments with and without the τ_{MS} feedback, it is found that the interactively represented τ_{MS}-SST_{MS} coupling can modulate the kinetic energy along the Kuroshio extension jet, with little effect on the Kuroshio pathway. Similar results are also obtained in three additional sensitivity experiments, which consider half strength of the τ_{MS}, and the momentum flux and heat flux effect induced by τ_{MS}, respectively. That means simply taking into account the τ_{MS}-SST_{MS} coupling has little effect on improving the simulation of the Kuroshio Current system.

Keyword: mesoscale wind stress-SST coupling; Kuroshio extension; surface kinetic energy; ocean modeling

1 INTRODUCTION

Significant mesoscale coupling perturbations (at a size of 100–1 000 km) in the ocean and atmosphere are observed in the Kuroshio Extension (e.g., Nonaka and Xie, 2003; Xie, 2004; Chelton et al., 2004; Maloney and Chelton, 2006; Small et al., 2008). For instance, the perturbed sea surface temperature (SST) is accompanied with perturbations in air temperature, cloud fraction, wind stress, and sea level pressure (e.g., Nonaka and Xie, 2003; Minobe et al., 2008; Tokinaga et al., 2009; Bryan et al., 2010). Mesoscale perturbations of SST (SST_{MS}) and sea surface wind stress (τ_{MS}) are positively correlated (e.g., Maloney and Chelton, 2006; Bryan et al., 2010; Chelton and Xie, 2010), suggesting that the τ_{MS} are driven by the SST_{MS}, by means of downward momentum transport and pressure adjustment (e.g., Small et al., 2008; Bryan et al., 2010; Frenger et al., 2013).

The mesoscale air-sea coupling has significant effect on both the atmosphere and ocean. On one hand, SST perturbations can directly affect the wind stress divergence and cloud fraction in the atmospheric boundary layer, and are hence important for precipitation simulations (e.g., Minobe et al., 2008; Putrasahan et al., 2013). On the other hand, the induced wind stress perturbations can in turn impact the oceanic conditions in the Kuroshio extension (e.g., Wei et al., 2017). Specifically, they can inhibit the mesoscale SST perturbations by means of surface heat flux and affect the local Ekman upwelling by means of momentum flux (e.g., Nonaka and Xie, 2003; Maloney and Chelton, 2006; Chelton, 2013;

* Supported by the National Natural Science Foundation of China (Nos. 41490644, 41490640), the “Transparent Ocean” Project (No. 2014GJJS0101), the National Key R&D Program of China (Nos. 2017YFC1404102, 2017YFC1404100), the Thousand Talents Plan (Long Term), the Taishan Scholarship, and the Aoshan Talents Program Supported by Qingdao National Laboratory for Marine Science and Technology (No. 2015ASTP)

** Corresponding author: rzhang@qdio.ac.cn

Wei et al., 2017).

The effect of mesoscale air-sea coupling on the oceanic jet has been previously studied from different methods. Ma et al. (2016) demonstrated that the mesoscale air-sea coupling had an effect of intensifying the Kuroshio based on the atmosphere-ocean coupled models. In their work, the effect of mesoscale air-sea coupling was isolated through comparing two experiments with and without the SST_{MS} before being used to force the atmosphere model. Using an idealized high-resolution quasi-geostrophic (QG) ocean model, Hogg et al. (2009) demonstrated that the mesoscale wind stress-SST coupling can reduce the strength of the ocean jet. These different results are probably caused by their different experimental settings. For instance, only the effect of τ_{MS}-SST_{MS} coupling is considered by Hogg et al. (2009), while all the atmospheric responses to SST_{MS} are taken into account by Ma et al. (2016). Thus, there are uncertainties in the effects of mesoscale air-sea coupling.

In Wei et al. (2017), we took a simple approach to incorporate the τ_{MS}-SST_{MS} coupling in the ocean model to study its effect on the oceanic conditions in the Kuroshio extension. This study continues to examine the effect of τ_{MS}-SST_{MS} coupling on the Kuroshio extension jet.

2 METHODOLOGY

2.1 Ocean model

The Regional Ocean Modeling System (ROMS) is employed to assess the effect of τ_{MS}-SST_{MS} coupling on the Kuroshio extension jet. The ROMS is a three-dimensional, hydrostatic, free-surface, terrain-following numerical model (e.g., Shchepetkin and McWilliams, 2005). The model domain is from 20°S to 60°N in latitude and from 100°E to 70°W in longitude. Longitude resolution is 1/8°, and latitude resolution is 1/8°×cos (latitude), with 50 s-coordinate levels in the vertical direction. The temperature, salinity, velocity, and surface elevation at boundaries are prescribed by spatial interpolation of the WOA2009 datasets. The 3D velocity, temperature, and salinity are nudged to boundary values at these three open lateral boundaries with a 360-day time scale for outflow and 3-day for inflow. The logical switches of nudging/relaxation are also turned on to nudge the 2D momentum and 3D temperature fields to their climatology with a 360-day time scale. The time steps are 30 s and 300 s for the 2-D and 3-D equations. At each time step, the surface net heat flux sensitivity to SST (dQ/dSST) is calculated and used to introduce thermal feedback to correct net surface heat flux (Barnier et al., 1995). More detailed descriptions of the model settings are given in Wei et al. (2017). After 20 year integration, a quasi-equilibrium state is obtained; and the derived oceanic variables in that time are used as initial conditions for experiments as described below.

Table 1 τ_{MS}-induced heat flux and momentum flux effects considered in five experiments

	No-feedback	Feedback	Half-feedback	MF-feedback	HF-feedback
Heat flux	-	1.0	0.5	-	1.0
Momentum flux	-	1.0	0.5	1.0	-

2.2 Numerical experiments

In order to assess the effect of τ_{MS}-SST_{MS} coupling, two experiments with and without the τ_{MS} feedback are carried out. In no-feedback experiment, the model settings are as normal. In the feedback experiment, the τ_{MS}-SST_{MS} coupling is incorporated in the model in the Kuroshio extension region.

The τ_{MS}-SST_{MS} coupling is incorporated into the ocean model by interactively determining the τ_{MS} from SST_{MS} following their close relationship. τ_{MS} is estimated from the equation: $\tau_{MS}=a\times SST_{MS}$, where a is regression coefficient and is taken 0.01 (Wei et al., 2017). The SST_{MS} simulated by the ocean model is isolated by using the locally weighted regression (loess) method (e.g., Cleveland and Devlin, 1988). In this study, a 10° latitude ×30° longitude loess spatial high-pass filter is used (Wei et al., 2017). The derived τ_{MS} is then used to combine with the climatology wind stress to force the ocean in the feedback experiment, with the amplitude changed from $|\tau|$ to $|\tau|+\tau_{MS}$, and the wind direction θ unchanged. The area where the τ_{MS}-SST_{MS} coupling is considered is located east of Japan, because the τ_{MS} and SST_{MS} are observed to be active there.

The τ_{MS} acts to impact the ocean by means of surface momentum flux and heat flux. In order to examine the sensitivity of the results to τ_{MS} and understand the way by which τ_{MS} impacts the ocean, three additional experiments are carried out. They are half-feedback experiment (which uses half strength of τ_{MS}), HF-feedback (τ_{MS} is allowed to influence the surface heat flux only) and MF-feedback (τ_{MS} is allowed to influence the surface momentum flux only) experiments (Table 1). In order to enhance

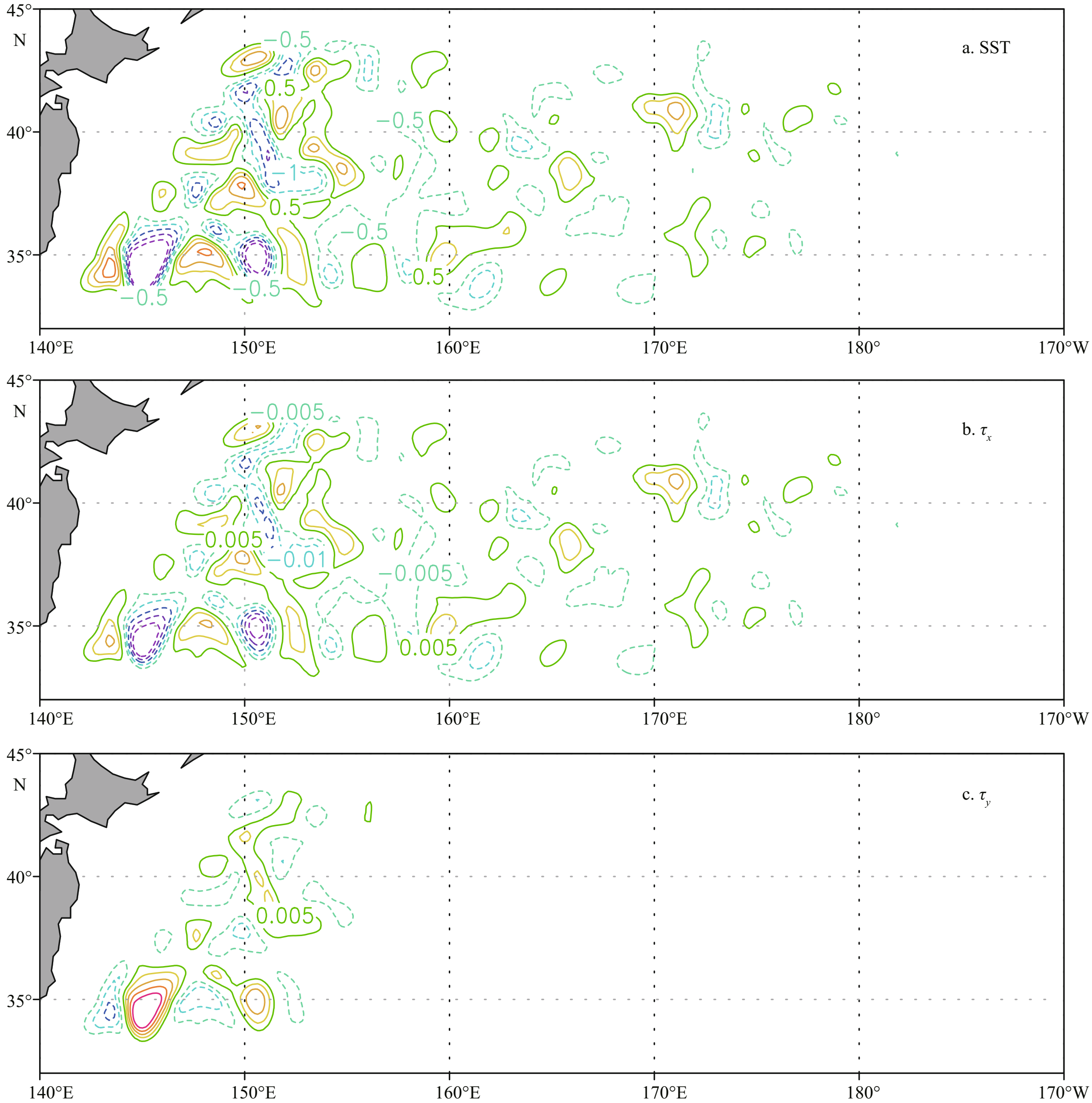

Fig.1 A snapshot of the SST_{MS} (unit: °C) simulated by the ocean model (a), and the zonal (b) and meridional (c) wind stress perturbations (unit: N/m^2) derived from it

computational speed, τ_{MS} is updated daily instead of instantly in all the above experiments. All the experiments are run for 10 years with monthly averaged output.

3 RESULT

3.1 The effectiveness of the empirical coupling

The high resolution model based on ROMS is eddy-permitting, even though wind stress forcing is climatology. As shown in Fig.1a, the simulated SST_{MS} has a size of about 100–400 km and an amplitude of about 2.5°C, which agree with that found in satellite observation (e.g., Wei et al., 2017). Figure 1b and c show the zonal and meridional mesoscale wind stress perturbations derived from the SST_{MS}. The spatial distribution of zonal wind stress perturbations agrees with that of SST_{MS}. The wind stress field perturbations are northwesterly in the area of positive SST_{MS} while southeasterly in the area of negative SST_{MS}, with the magnitude at about 0.03 N/m^2. Therefore, the mesoscale wind stress field perturbations can be derived from the empirical relationship with respect to SST_{MS}.

Positive correlation between τ_{MS} and SST_{MS} is obtained after incorporation of the τ_{MS}-SST_{MS} coupling

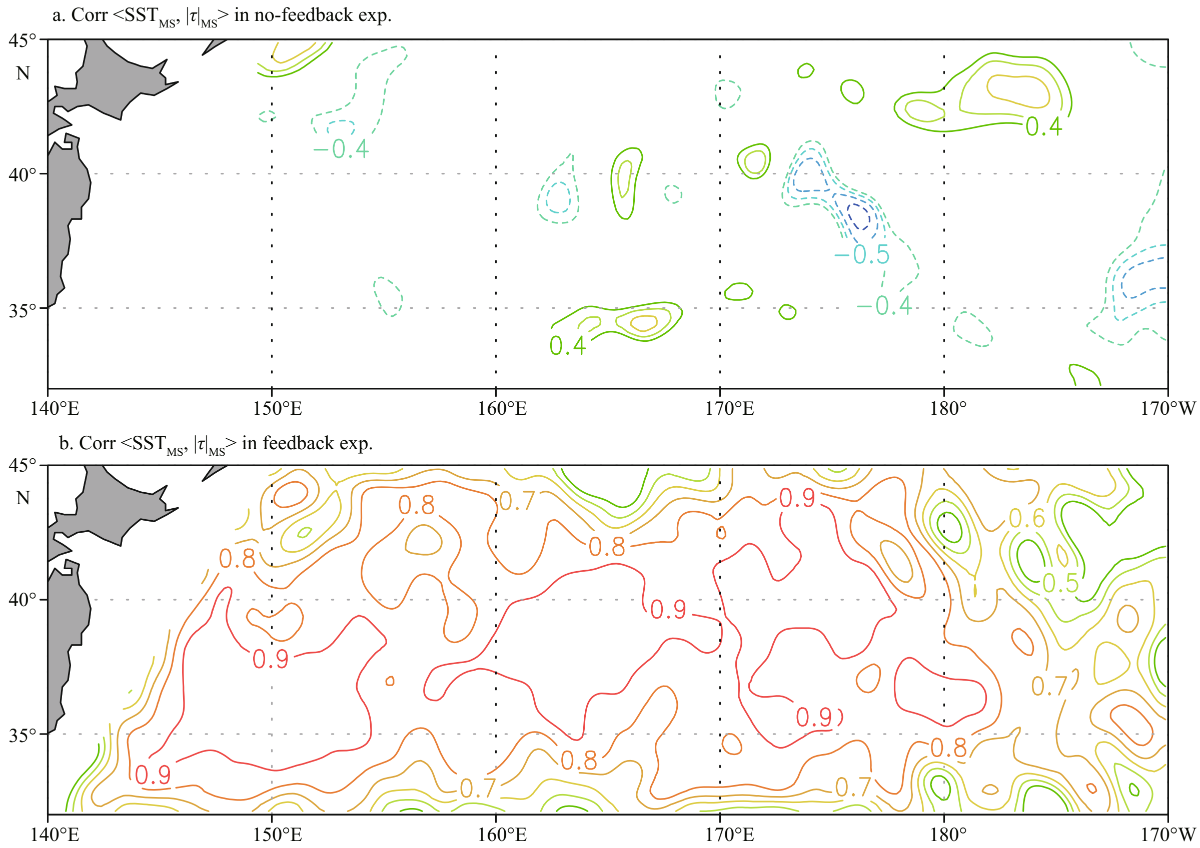

Fig.2 Correlation coefficients between SST_{MS} and τ_{MS} in no-feedback (a) and feedback (b) experiments

Contour interval is 0.1, with small value (<0.4) contours omitted.

(Fig.2). Correlation coefficient between τ_{MS} and SST_{MS} was often simulated incorrectly in the low resolution climate models (e.g., Maloney and Chelton, 2006; Bryan et al., 2010). This problem exists in the no-feedback experiment when the τ_{MS} is not incorporated into the ocean model (Fig.2a). The incorporation of the empirical τ_{MS}-SST_{MS} coupling helps to improve this problem, and enhances the correlation between them (Fig.2b). These results altogether suggest that the empirical τ_{MS}-SST_{MS} coupling utilized here is effective to capture their inherent relationship.

3.2 Effect on the Kuroshio extension jet

The τ_{MS}-SST_{MS} coupling is interactively incorporated into the model to represent the τ_{MS} feedback on the ocean. In this subsection, the effect of τ_{MS} on the Kuroshio extension jet is isolated through comparing two experiments with and without it. Figure 3a and b show the mean kinetic energy simulated by no-feedback and feedback experiments as averaged from year 21 to 30. The kinetic energy can reach 2.0 m^2/s^2, suggesting that the Kuroshio velocity can reach 1.4 m/s. Significant kinetic energy difference between two experiments is seen along the Kuroshio extension jet (Fig.3c); the largest difference exceeds 0.2 m^2/s^2, which is about 10% of the mean kinetic energy.

Figure 3d–f show corresponding distance-depth cross-sections of zonal velocities simulated by no-feedback and feedback experiments averaged from 142°E to 152°E, and their difference. It is seen that the Kuroshio Current can reach to a depth of 1 500 m, with relatively weak counter current on its two flanks (Fig.3d). The position of the Kuroshio extension jet is almost unchanged compared with that in the no-feedback experiment (Fig.3e). The velocity difference between no-feedback and feedback experiments is negative at the Kuroshio axis, while positive at its two sides (Fig.3f). The difference with the same sign can reach to a depth of 2 000 m. These results suggest that the τ_{MS}-SST_{MS} coupling can modulate the Kuroshio velocity, while has little effect on the position of the Kuroshio pathway (Fig.3d and e).

The kinetic energy differences in half-feedback, MF-feedback and HF-feedback experiments relative

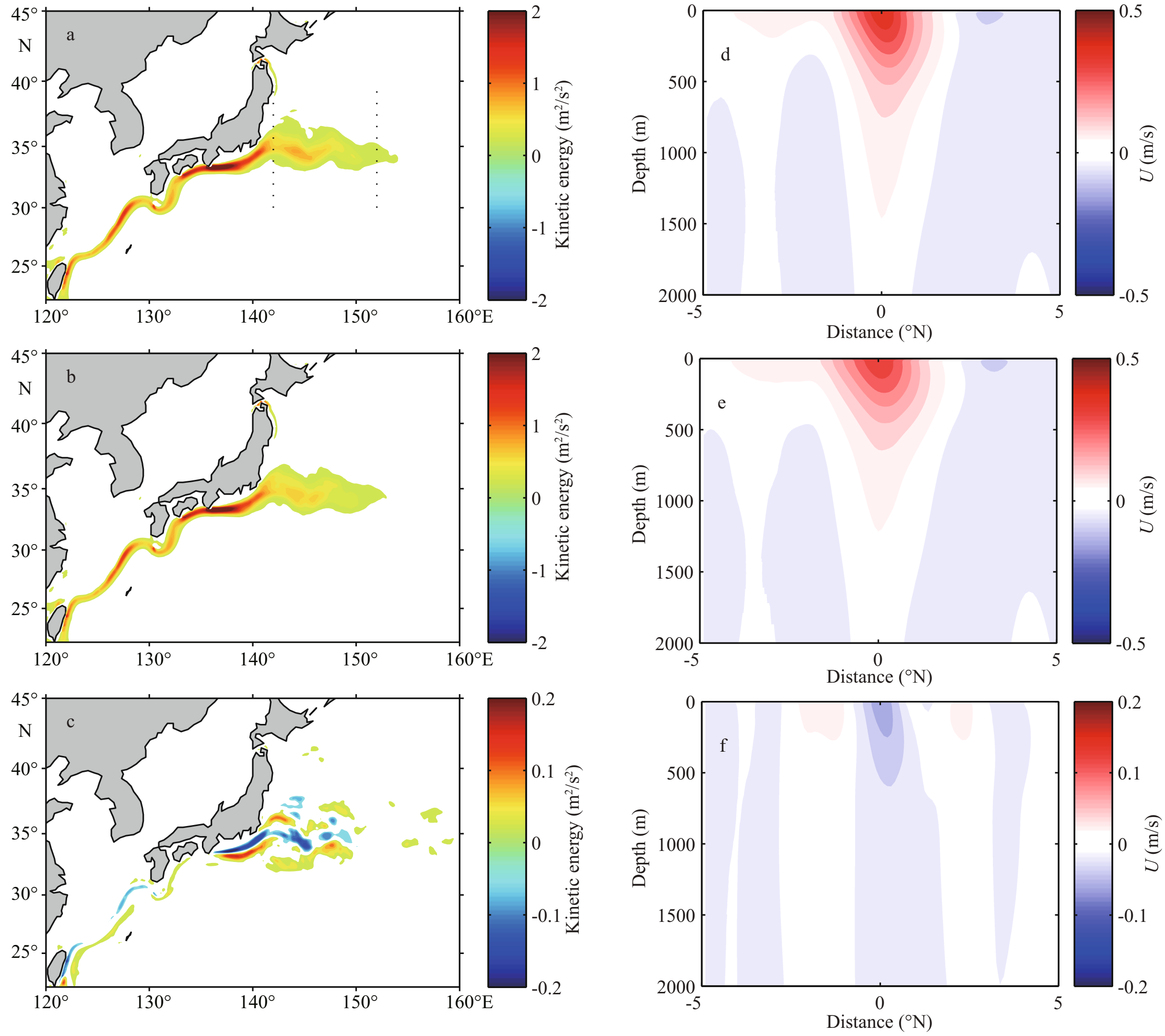

Fig.3 The surface kinetic energy (unit: m²/s²) simulated in no-feedback (a) and feedback (b) experiments, and their difference (c); the corresponding zonal velocity (unit: m/s) averaged from 142°E to 152°E are shown in (d), (e), and (f)

The *x* axis in d–f denotes the distance from the Kuroshio axis (0), with negative (positive) values indicating distances north (south) of the Kuroshio jet. All results are averaged from the model year 21 to 30.

to that in the no-feedback experiment are shown in Fig.4. It is seen that the kinetic energy has substantial changes along the Kuroshio extension jet in these experiments. The results suggest that the τ_{MS}-SST_{MS} coupling acts to affect the Kuroshio surface kinetic energy through either the way of moment flux or heat flux. However, the position of the Kuroshio extension jet is not found to change systematically in these experiments. It can be also found that the magnitude of surface kinetic energy difference in the half-feedback experiment (Fig.4a) is not significantly reduced relative to that in the feedback experiment (Fig.3c), suggesting that the kinetic energy difference might be not linearly related to the strength of τ_{MS}. Moreover, the surface kinetic energy difference in the feedback experiment (Fig.3c) seems to be not a simple combination of the differences caused respectively by the effects of surface heat flux and momentum flux (Fig.4b and c).

The effects of τ_{MS}-SST_{MS} coupling are also seen in the SST, wind stress curl and surface heat flux. Figure 5a shows the SST difference between no-feedback and feedback experiments as averaged over the model year 21–30. It is seen that the SST difference can reach 0.3°C, but in a structure that is very patchy. Figure 5b shows the wind stress curl difference between two experiments. The difference in wind stress curl between the two experiments is about 0.5×10^{-7} N/m³, which is a small portion (about 10%) relative to the observed mesoscale wind stress curl perturbations (e.g., Wei et al., 2017). Figure 5c shows the surface net heat flux (downward positive)

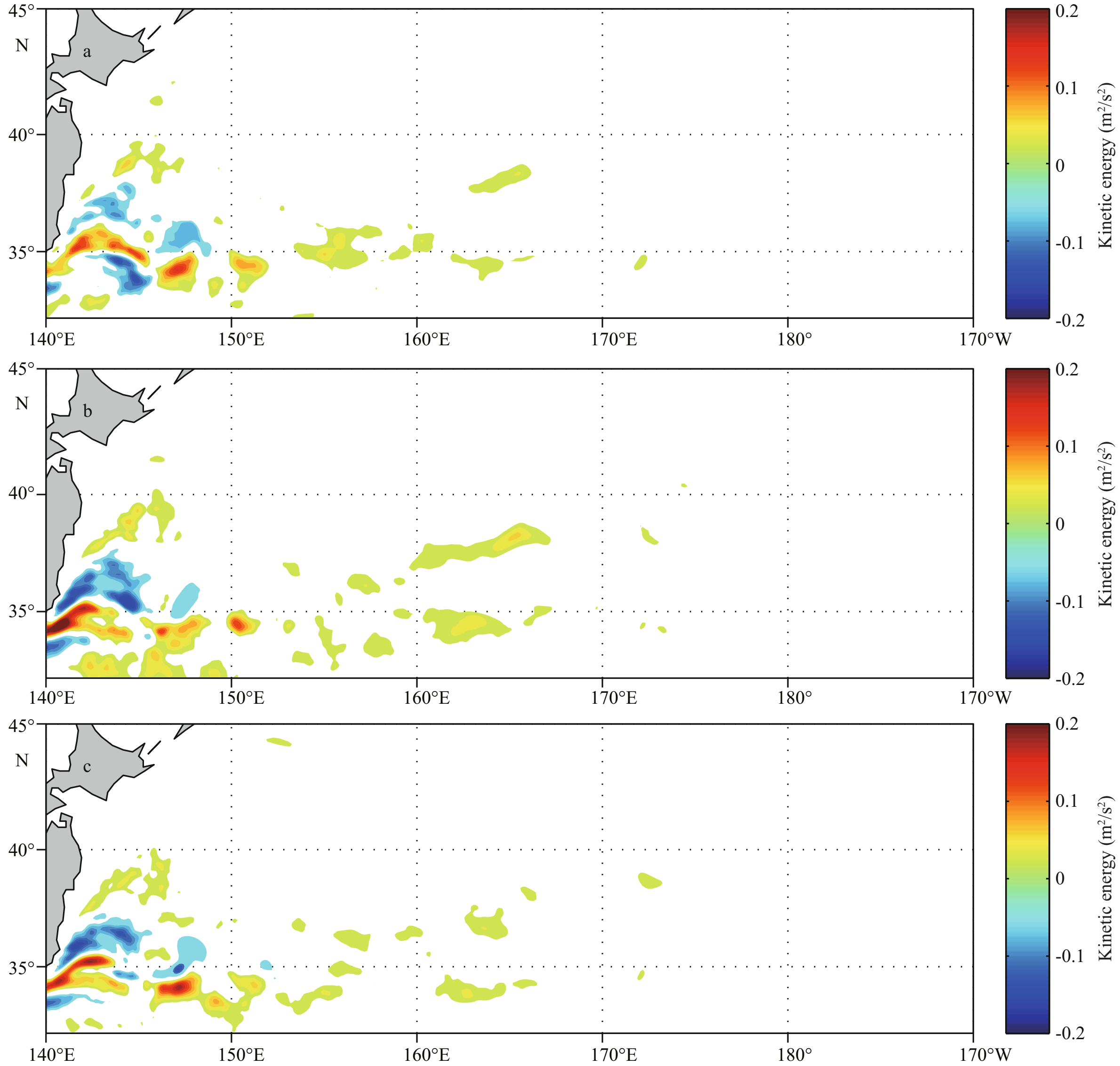

Fig.4 The surface kinetic energy differences (relative to no-feedback experiment) in half-feedback (a), MF-feedback (b) and HF-feedback (c) experiments averaged from the model year 21 to 30

difference between the two experiments, which has a magnitude of about 15 W/m^2.

An interesting phenomenon is that the τ_{MS} induced kinetic energy difference is small east of 150°E (Fig.3c), although there are large surface net heat flux, SST, and wind stress curl differences (Fig.5). That means the kinetic energy difference is not simply caused by the differences of these three terms. As the Kuroshio speed is large, a small change in the Kuroshio extension jet (e.g., intrinsic fluctuations) might results in large difference in the surface kinetic energy. For instance, the wind stress curl induced Ekman pumping might interact with the Kuroshio and result in the distinct kinetic energy difference along the Kuroshio pathway.

4 CONCLUDING REMARKS

The effect of mesoscale wind stress-SST coupling on the Kuroshio extension jet is investigated by using a high resolution ocean model. The perturbed sea surface wind stress field is estimated empirically from modeled SST_{MS} and then incorporated into the ocean model. The effect of τ_{MS}-SST_{MS} coupling on the Kuroshio extension jet is isolated through comparing two experiments with and without this effect. It is found that the τ_{MS}-SST_{MS} coupling can substantially affect the surface kinetic energy along the Kuroshio extension jet, with little effect on the climatology mean position of the Kuroshio pathway. Further sensitivity analyses suggest that the τ_{MS} can affect the

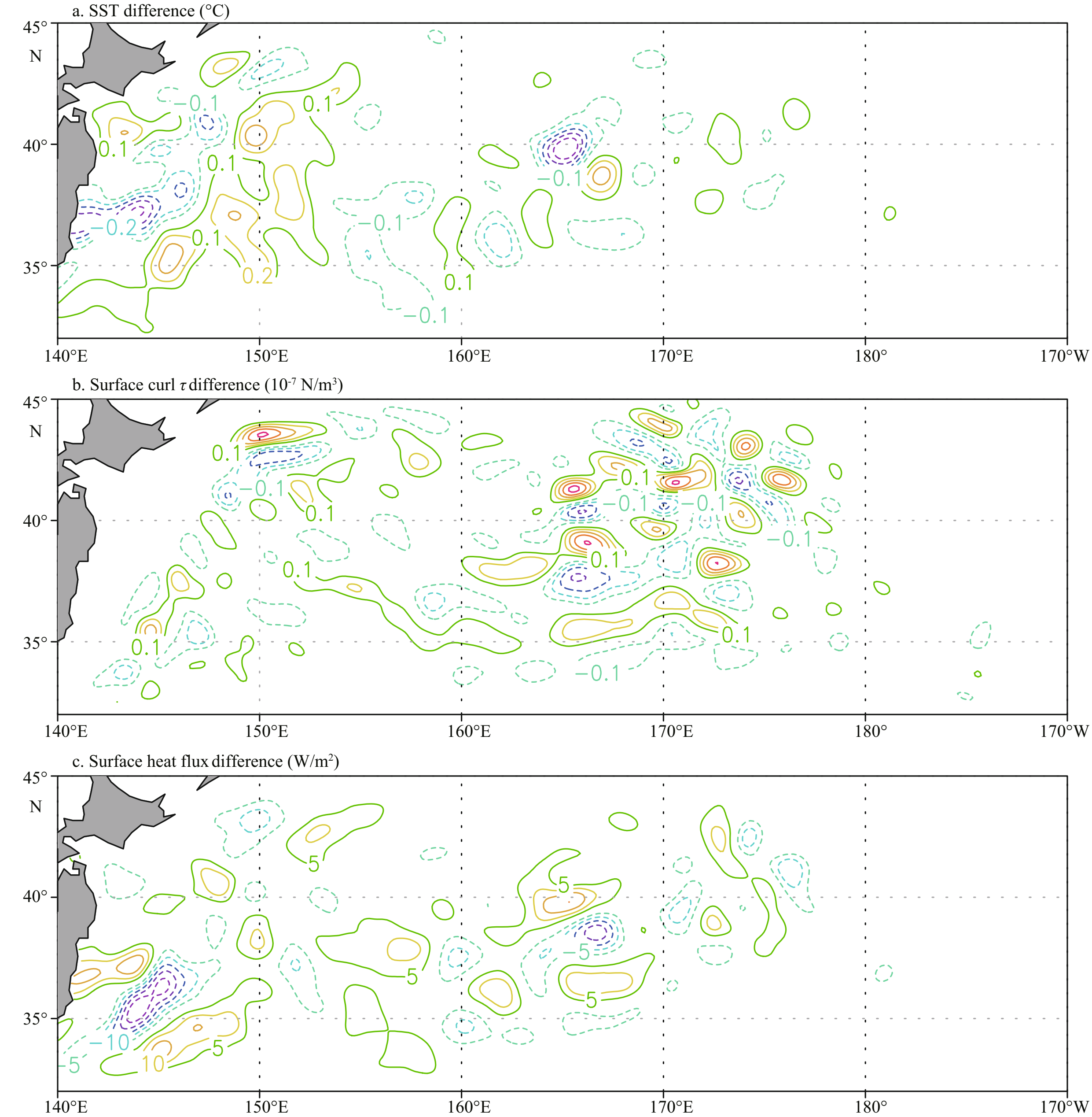

Fig.5 SST (a), wind stress curl (b) and surface heat flux (c) differences between no-feedback and feedback experiments as averaged from year 21 to 30

Positive curl value indicates upwelling, while negative value indicates downwelling. Surface heat flux is negative while the ocean loses heat.

surface kinetic energy from either the way of surface heat flux or momentum flux. The interactively represented τ_{MS}-SST_{MS} coupling also affects the climatology mean SST, wind stress curl and surface heat flux, but the induced differences are all very patchy.

Hogg et al. (2009) pointed out that the τ_{MS}-SST_{MS} coupling can reduce the strength of the ocean jet using a high-resolution quasigeostrophic ocean model. Ma et al. (2016) pointed out that the mesoscale air-sea coupling can enhance the strength of the Kuroshio extension jet and affect the position of the Kuroshio axis. These different results arise from different models and ways used to isolate the effect of mesoscale air-sea coupling. Hogg et al. (2009) examined the effect of τ_{MS}-SST_{MS} coupling from an idealized ocean model. Ma et al. (2016) isolated the effect of mesoscale air-sea coupling by utilizing the atmosphere-ocean coupled models, by comparing two experiments with and without the SST_{MS} component before being provided to the atmosphere model. The approach used by Ma et al. (2016) is advantageous over many aspects; however, the induced large scale atmospheric changes might also interface in their results. In relative, our current study isolated the effect of τ_{MS}-SST_{MS} coupling in a cleaner way. This study demonstrates that the kinetic energy difference between no-feedback and feedback experiments is large in vicinity of the Kuroshio, which might be linked to interactions between small scale oceanic disturbances and the Kuroshio. This study shows that there is no change in the Kuroshio pathway (Fig.3a and b) after incorporation of τ_{MS}-SST_{MS} coupling.

The results derived in this study have some implications on the climate model biases. The long term mean SST difference induced by τ_{MS} is patchy (Fig.5a), so that it could not account for the systematic SST biases appeared in climate models. Moreover, the τ_{MS}-SST_{MS} coupling is not found to affect the position of the long term mean Kuroshio extension jet, so that it has little effect on improving the simulations of the Kuroshio Current system.

References

Barnier B, Siefridt L, Marchesiello P. 1995. Thermal forcing for a global ocean circulation model using a three-year climatology of ECMWF analyses. *Journal of Marine Systems*, **6**(4): 363-380.

Bryan F O, Tomas R, Dennis J M et al. 2010. Frontal scale air-sea interaction in high-resolution coupled climate models. *Journal of Climate*, **23**(23): 6 277-6 291.

Chelton D B, Schlax M G, Freilich M H, Milliff R F. 2004. Satellite measurements reveal persistent small-scale features in ocean winds. *Science*, **303**(5660): 978-983.

Chelton D B, Xie S P. 2010. Coupled ocean-atmosphere interaction at oceanic mesoscales. *Oceanography*, **23**(4): 52-69.

Chelton D. 2013. Ocean-atmosphere coupling: mesoscale eddy effects. *Nature Geoscience*, **6**(8): 594-595.

Cleveland W S, Devlin S J. 1988. Locally weighted regression: an approach to regression analysis by local fitting. *Journal of the American Statistical Association*, **83**(403): 596-610.

Frenger I, Gruber N, Knutti R et al. 2013. Imprint of Southern Ocean eddies on winds, clouds and rainfall. *Nature Geoscience*, **6**(8): 608-612.

Hogg A M C, Dewar W K, Berloff P, Kravtsov S, Hutchinson D K. 2009. The effects of mesoscale ocean-atmosphere coupling on the large-scale ocean circulation. *Journal of Climate*, **22**(15): 4 066-4 082.

Ma X H, Jing Z, Chang P et al. 2016. Western boundary currents regulated by interaction between ocean eddies and the atmosphere. *Nature*, **535**(7613): 533-537.

Maloney E D, Chelton D B. 2006. An assessment of the sea surface temperature influence on surface wind stress in numerical weather prediction and climate models. *Journal of Climate*, **19**(12): 2 743-2 762.

Minobe S, Kuwano-Yoshida A, Komori N, Xie S P, Small R J. 2008. Influence of the Gulf Stream on the troposphere. *Nature*, **452**(7184): 206-209.

Nonaka M, Xie S P. 2003. Covariations of sea surface temperature and wind over the Kuroshio and its extension: evidence for ocean-to-atmosphere feedback. *Journal of Climate*, **16**(9): 1 404-1 413.

Putrasahan D A, Miller A J, Seo H. 2013. Isolating mesoscale coupled ocean–atmosphere interactions in the Kuroshio Extension region. *Dynamics of Atmospheres and Oceans*, **63**: 60-78.

Shchepetkin A F, McWilliams J C. 2005. The regional oceanic modeling system (ROMS): a split-explicit, free-surface, topography-following-coordinate oceanic model. *Ocean Modelling*, **9**(4): 347-404.

Small R J, de Szoeke S P, Xie S P et al. 2008. Air-sea interaction over ocean fronts and eddies. *Dynamics of Atmospheres and Oceans*, **45**(3-4): 274-319.

Tokinaga H, Tanimoto Y, Xie S P, Sampe T, Tomita H, Ichikawa H. 2009. Ocean frontal effects on the vertical development of clouds over the western North Pacific: in situ and satellite observations. *Journal of Climate*, **22**(16): 4 241-4 260.

Wei Y Z, Zhang R H, Wang H N. 2017. Mesoscale wind stress-SST coupling in the Kuroshio Extension and its effect on the ocean. *Journal of Oceanography*, https://doi.org/10.1007/s10872-017-0432-2. (in press)

Xie S P. 2004. Satellite observations of cool ocean-atmosphere interaction. *Bulletin of the American Meteorological Society*, **85**(2): 195-208.